Computer Assisted Methods in Engineering and Science, **21**: 113–121, 2014.

Trabecular bone numerical homogenization with the use of buffer zone

Przemysław Makowski, Wacław Kuś
Institute of Computational Mechanics and Engineering
Silesian University of Technology, Konarskiego 18A, 44-100 Gliwice, Poland
e-mail: przemyslaw.makowski@polsl.pl, waclaw.kus@polsl.pl

The paper is devoted to calculation of effective orthotropic material parameters for trabecular bone tissue. The finite element method (FEM) numerical model of bone sample was created on the basis of micro-computed tomography (μCT) data. The buffer zone surrounding the tissue was created to apply the periodic boundary conditions. Numerical homogenization algorithm was implemented in FEM software and used to calculate the elasticity matrix coefficients of the considered bone sample.

Keywords: trabecular bone, numerical homogenization, multiscale modeling, FEM.

1. Introduction

Trabecular bone is a bone tissue located mainly inside the epiphyses of long bones, for example at the end of human femur (Fig. 1). Trabecular bone is an orthotropic material because of its microstructure geometry that is the spatial organization of bone trabeculas at the micro scale [21]. The orthotropic character of the bone plays a crucial role in understanding of the mechanical behavior of the whole bone at the macro scale. Material parameters of bone can be obtained on the basis of experimental tests (usually compression test), fabric measurements (e.g., mean intercept length – MIL) or numerical simulations using models taking into account the microstructure of the bone sample. In work [20] the authors used FEM numerical models of trabecular bone microstructure and compared obtained material parameters with values calculated on the basis of fabric measurements, finding a good correlation ($R^2 > 0.92$).

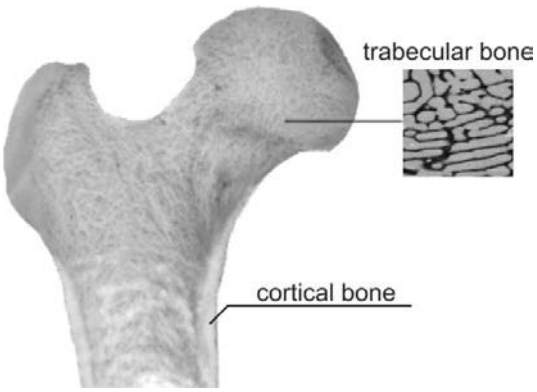

Fig. 1. Structure of human femur epiphysis.

Experimental evaluation of the bone material parameters, both at micro and macro scales is very difficult and usually subjected to large errors. At the macro scale, experimental errors are

related mainly to boundary artifacts caused by extraction of the bone sample from its environment – the surrounding bone tissue. At the micro scale, the experimental errors are related to a small size of single trabecula. These difficulties are reflected by a very wide range of tissue modulus (from 1 GPa to even 20 GPa) reported in [10]. To overcome problems related micro-scale experimental measurements, the numerical simulations and the effective isotropic tissue modulus concept can be used. Although the trabecular tissue – the bone's trabeculas – is heterogeneous and anisotropic, the influence of these characteristics on the effective orthotropic elastic properties of the bone at the macro level is negligible [7]. At the macro-scale the boundary artifacts can be reduced using μFEM models of bone sample and numerical simulations of experimental tests. In case of compression test simulations, although the bending of trabeculas cut at the boundary of the sample can be eliminated by applying the appropriate boundary conditions, the structure can still freely expand in directions perpendicular to the compression axis. In this study, to ensure the conditions close to the bone in vivo environment, the periodic boundary conditions (PBC) are applied to the numerical model of trabecular bone's cubical sample. Use of periodic boundary conditions for the locally periodic trabecular bone structure can reduce the boundary artifacts and eliminate underestimation or overestimation of the elastic properties occurring when using other BCs. Periodic boundary conditions can simulate the actual environment of considered bone sample which in vivo is surrounded by bone tissue.

The use of FEM numerical models built on the basis of micro-tomography data segmentation allows one to take into account the real microstructure of bone tissue. By using such numerical models, one can calculate macro-scale orthotropic parameters of the bone using homogenization methods and periodic boundary conditions. The orthotropic material parameters of bone can be used in the design of the optimized, patient specific hip joint endoprosthesis and bone scaffolds [4, 5].

2. Multiscale modeling of structures

Biological and engineering materials exhibit different structure depending on the observation scale. At the micro scale, trabecular bone is a heterogeneous structure composed of interconnected bone trabeculas. At the macro scale (at least five inter-trabecular lengths), trabecular bone can be considered as a homogeneous structure with effective material parameters. In the case of multiscale modeling, the analyses are performed at different scales (Fig. 2) – for example at the micro and the macro scale, to obtain the relationship between the microstructure and the macro-scale effective material parameters of the structure. The orthotropic character of trabecular bone is an effect of trabecular alignment – the microstructure of the bone.

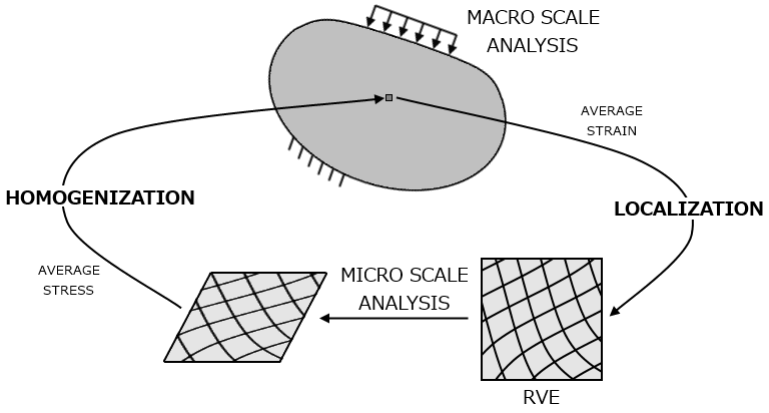

Fig. 2. Idea of Multiscale modeling.

Multiscale modeling can be performed using bridging techniques or homogenization methods [2, 3, 11]. The idea behind the homogenization is the replacement of a heterogeneous material by an

equivalent homogenous material with effective material parameters (Fig. 3). This method utilizes the concept of representative volume element (RVE) which is considered as the smallest volume of the medium comprising all the needed information about the structure and parameters of the whole material. In this study, the FEM numerical model of trabecular bone sample is considered as an RVE model of the bone structure.

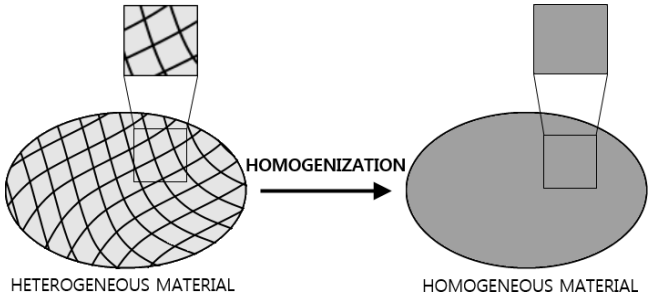

Fig. 3. Homogenization.

Trabecular bone is a locally periodic structure (Fig. 4). The periodic boundary conditions (PBC) are applied in the RVE model, so periodic displacements $\mathbf{u}$ (1) and anti-periodic tractions $\mathbf{t}$ (2) are enforced on the opposite boundaries of the RVE model (Fig. 5).

$$\mathbf{u}^{+} = \mathbf{u}^{-}, \tag{1}$$

$$\mathbf{t}^{+} = -\mathbf{t}^{-}. \tag{2}$$

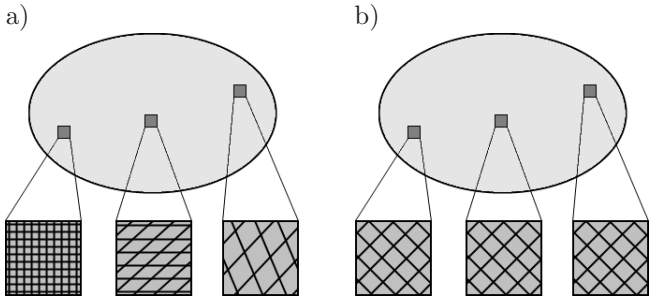

Fig. 4. Example of a) locally periodic structure, b) globally periodic structure.

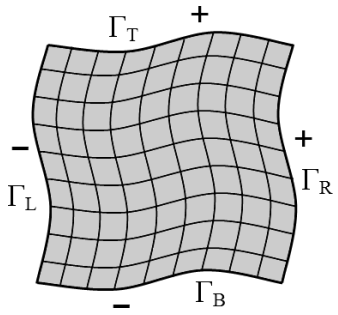

Fig. 5. Periodic boundary conditions.

The transition from the micro scale (RVE model) to the macro scale (effective material parameters) is based on averaging of the stresses (3) and strains (4) in the RVE model.

$$\langle \sigma_{ij} \rangle = \frac{1}{V_{\mathrm{RVE}}} \int\limits_{\Omega_{\mathrm{RVE}}} \sigma_{ij}\, d\Omega_{\mathrm{RVE}}, \tag{3}$$

where $\langle\sigma_{ij}\rangle$ – averaged stress at the macro scale, σ_{ij} – stresses at the micro scale (RVE), V_{RVE} – RVE volume

$$\langle\varepsilon_{ij}\rangle = \frac{1}{V_{\mathrm{RVE}}} \int\limits_{\Omega_{\mathrm{RVE}}} \varepsilon_{ij}\, d\Omega_{\mathrm{RVE}}, \tag{4}$$

where $\langle\varepsilon_{ij}\rangle$ – averaged strain at the macro scale, ε_{ij} – strains at the micro scale (RVE), V_{RVE} – RVE volume.

The averaged stresses are calculated through numerical integration over finite elements Gauss points. In the case of 3D linear elastic problems, calculating the material parameters of the equivalent homogeneous material (effective material parameters) requires solving six boundary value problems for the RVE model subjected to six unit strains with periodic boundary conditions. The result of these calculations is the elasticity matrix $\mathbf{C}$ of the equivalent homogeneous material, binding the averaged stresses and strains.

The constitutive relationship for linear elastic orthotropic material in Voigt notation is formulated as

$$\langle\sigma_{ij}\rangle = \mathbf{C}\langle\varepsilon_{ij}\rangle, \tag{5}$$

$$\begin{bmatrix} \langle\sigma_{11}\rangle \\ \langle\sigma_{22}\rangle \\ \langle\sigma_{33}\rangle \\ \langle\sigma_{12}\rangle \\ \langle\sigma_{23}\rangle \\ \langle\sigma_{31}\rangle \end{bmatrix} = \begin{bmatrix} c_{11} & c_{12} & c_{13} & 0 & 0 & 0 \\ & c_{22} & c_{23} & 0 & 0 & 0 \\ & & c_{33} & 0 & 0 & 0 \\ & \text{sym.} & & c_{44} & 0 & 0 \\ & & & & c_{55} & 0 \\ & & & & & c_{66} \end{bmatrix} \begin{bmatrix} \langle\varepsilon_{11}\rangle \\ \langle\varepsilon_{22}\rangle \\ \langle\varepsilon_{33}\rangle \\ \langle\varepsilon_{12}\rangle \\ \langle\varepsilon_{23}\rangle \\ \langle\varepsilon_{31}\rangle \end{bmatrix}. \tag{6}$$

For orthotropic materials, there are nine non-zero independent coefficients of elasticity matrix due to its symmetry. Elasticity matrix $\mathbf{C}$ can be then applied as an effective material parameter of the homogenized structure in any commercial FEM software. The engineering constants can be obtained on the basis of Eq. (7):

$$\mathbf{S} = \mathbf{C}^{-1} = \begin{bmatrix} \frac{1}{E_1} & \frac{-\nu_{21}}{E_2} & \frac{-\nu_{31}}{E_3} & 0 & 0 & 0 \\ \frac{-\nu_{12}}{E_1} & \frac{1}{E_2} & \frac{-\nu_{32}}{E_3} & 0 & 0 & 0 \\ \frac{-\nu_{13}}{E_1} & \frac{-\nu_{23}}{E_2} & \frac{1}{E_3} & 0 & 0 & 0 \\ 0 & 0 & 0 & \frac{1}{G_{23}} & 0 & 0 \\ 0 & 0 & 0 & 0 & \frac{1}{G_{31}} & 0 \\ 0 & 0 & 0 & 0 & 0 & \frac{1}{G_{12}} \end{bmatrix}, \tag{7}$$

where $\mathbf{S}$ – compliance matrix, E_i – Young's modules, G_{ij} – shear modules, ν_{ij} – Poisson's ratios.

3. Discrete numerical model of bone tissue

The orthotropic character of bone results from the tissue microstructure – spatial arrangement of bone trabeculas. Although scanning of human femur epiphysis with the use of microtomograph is possible, the process of μCT data segmentation and further remeshing of FEM model is not only difficult, but also time consuming. More importantly, time needed for calculating such a numerical model will make further identification and optimization tasks impossible. Calculation time, however, can be significantly reduced using multiscale approach and RVE models [13].

The cubical sample of trabecular bone with edge length value 10 mm was extracted from the head of human femur with accordance to anatomical axes – the characteristic patterns of trabecular alignment and density. Bone sample was scanned with use of Phoenix v|tome|x microtomograph [1]. The bone volume to total volume (BT/TV) value calculated on the basis of μCT data is equal to 45% – a relatively high value for trabecular bone. The FEM numerical model of the bone sample microstructure (Fig. 6) was created using Materialise MIMICS software. The final model, after remeshing, consists of about 800 thousand four-node, linear shape function tetrahedral finite elements (Fig. 6). The modeling of the whole bone, interaction with implants and scaffolds, however, cannot be performed with such a high level of details.

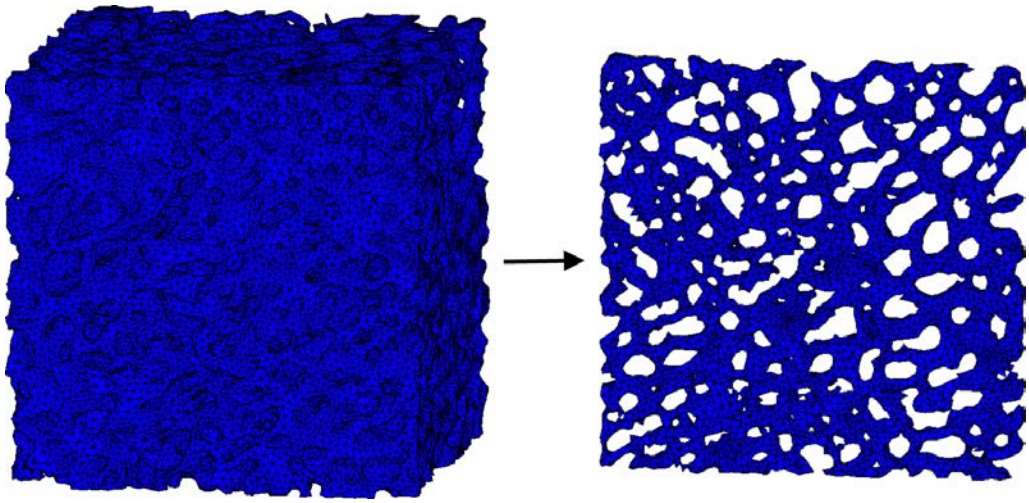

Fig. 6. Numerical model of trabecular bone sample and one of the cross sections.

After the μCT scanning the considered bone sample was tested experimentally [8, 9] (compression test using MTS Insight test machine). Compression test was then simulated with boundary conditions as close as possible to the experimental setup. Then isotropic material parameters of bone trabeculas (micro-scale parameters) constituting the structure of sample were identified with the evolutionary identification methods using experimental data and simulation results [14]. Obtained results of identification – Young's modulus and Poisson's ratio of trabeculas – were validated using nanoindentation method, finding a good correlation between them [8].

4. Periodic boundary conditions for non-periodic meshes

The RVE can be analyzed with the use of displacement, traction or periodic boundary conditions. The displacement boundary conditions overestimate and traction boundary conditions underestimate the calculated values of effective material parameters. The use of the periodic boundary conditions gives most accurate estimates of effective stiffness, bounded always between values obtained using other boundary conditions [16].

The application of the periodic boundary conditions with the use of multi-point constraints (MPC), in the case of RVE models with similar, regular meshes on the opposite sides of RVE, can be easily performed. However, applying of PBCs to irregular and porous, complicated RVE models of the real trabecular bone microstructure is not possible. This problem can be overcome by building the buffer zone [15] that surrounds the specimen model (Fig. 7). The buffer zone is the place of the transition from irregular tissue mesh to the regular boundary mesh. Use of the buffer zone allows one to obtain identical meshes on the opposite boundary faces of RVE model and to apply the periodic boundary conditions.

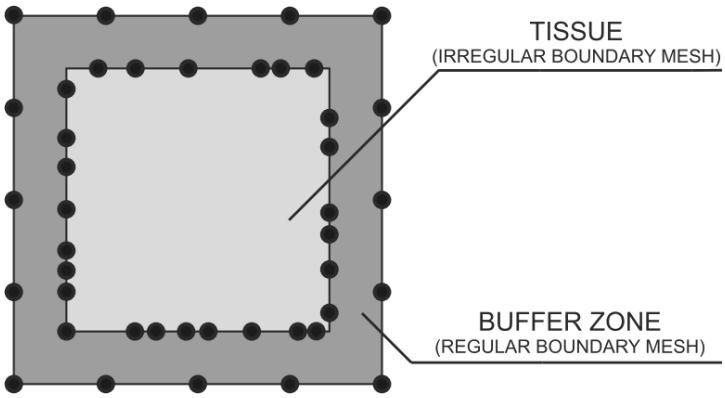

Fig. 7. Idea of Buffer zone.

The large size of the zone buffer zone results in error of calculated effective material parameters [15], but on the other hand the thickness should be sufficient to allow the mesh transition. The buffer zone thickness for the bone sample considered in this paper was chosen to be 10% of the size of RVE. The numerical model of bone microstructure surrounded by the buffer zone (Fig. 8) with applied periodic boundary conditions is used to calculate effective material parameters of bone tissue.

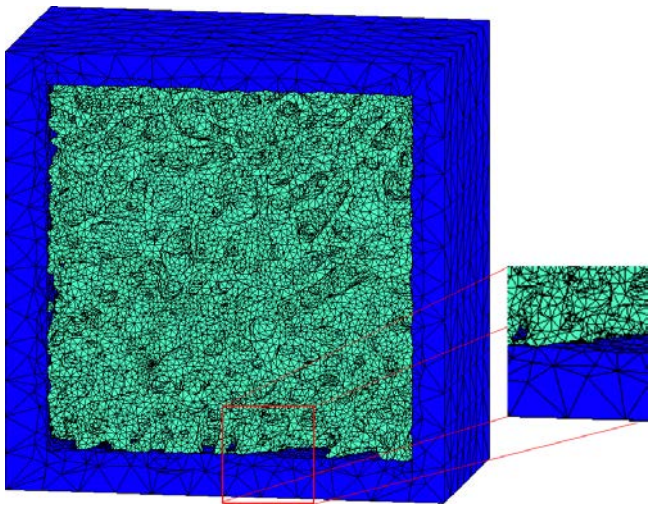

Fig. 8. Half of the RVE model with surrounding buffer zone.

5. Effective material parameters of the bone tissue

First, the isotropic material model for buffer zone is used with values of elastic parameters based on the performed compression test experiment ($E = 1148$ MPa). The trabeculas material properties were identified for the considered sample [14], Young's modulus and Poisson's ratio are respectively $E_{\mathrm{TRAB}} = 7895$ MPa and $\nu_{\mathrm{TRAB}} = 0.36$. The parameters of a single trabecula are isotropic but due to the geometrical structure of the RVE, the effective material properties are orthotropic. Six unit strains are applied into tissue area to calculate effective material parameters of bone using numerical homogenization method.

The analyses and simulations were performed using the MSC.Marc FEM software. Numerical homogenization algorithm was implemented in MSC.Marc software using user subroutines coded in Fortran [12]. The calculations time for each case of unit strain applied to RVE model was approximately 2.5 hours on a computer with processor Intel i3 3 Ghz, 4 GB RAM.

The result of calculations is the elasticity matrix $\mathbf{C}$ of bone sample:

$$\mathbf{C} = \begin{bmatrix} 1896.975 & 510.523 & 566.842 & 55.171 & -9.371 & -22.603 \\ & 1684.765 & 513.809 & 35.655 & -25.572 & 0.454 \\ & & 2453.461 & 20.115 & -48.886 & -35.507 \\ & \text{sym.} & & 443.817 & -3.688 & -10.968 \\ & & & & 466.048 & 15.899 \\ & & & & & 490.968 \end{bmatrix}. \tag{8}$$

Coefficients with values of at least one order of magnitude lower than the average value of parameters are listed in grey. Because trabecular bone is not a perfectly orthotropic material, these non-zero coefficients will remain. Moreover, sample was extracted with accordance to main anatomical axes (patterns of trabecular alignment and density visible on X-ray images) in femur epiphysis, which are supposed to be aligned with main directions of orthotropy, but the small error in specimen extraction will always remain.

To reduce the inevitable error in specimen extraction, the coordinate transformation that yields best orthotropic representation $\mathbf{C^{ORT}}$ (9) of the elasticity matrix was performed.

$$\mathbf{C^{ORT}} = \begin{bmatrix} c_{11} & c_{12} & c_{13} & \delta_{14} & \delta_{15} & \delta_{16} \\ & c_{22} & c_{23} & \delta_{24} & \delta_{25} & \delta_{26} \\ & & c_{33} & \delta_{34} & \delta_{35} & \delta_{36} \\ & \text{sym.} & & c_{44} & \delta_{45} & \delta_{46} \\ & & & & c_{55} & \delta_{56} \\ & & & & & c_{66} \end{bmatrix}, \tag{9}$$

where δ_{ij} is small number.

The initial coordinate system is rotated by three angles about x, y and z axis. The elasticity matrices, before and after transformation, are related by the transformation matrix $\mathbf{R}$ shown in Eq. (10) (summation notation used) [19]:

$$\widetilde{\mathbf{C}}_{ijkl} = \mathbf{R}_{i\alpha}\mathbf{R}_{j\beta}\mathbf{R}_{k\gamma}\mathbf{R}_{l\delta}\widetilde{\mathbf{C}}_{\alpha\beta\gamma\delta}, \tag{10}$$

where $\widetilde{\mathbf{C}}_{\alpha\beta\gamma\delta}$ – initial elasticity matrix in tensor notation, $\widetilde{\mathbf{C}}_{ijkl}$ – transformed elasticity matrix in tensor notation, $\mathbf{R}$ – transformation matrix containing transformation angles.

Evolutionary algorithm is used to minimize the objective function (11) to find the best orthotropic representation of bone sample elasticity matrix (8).

$$F(\mathbf{ch}) = \frac{\sum_{i=1}^{6}\sum_{j=1}^{6}\delta_{ij}^2}{\sum_{i=1}^{6}\sum_{j=1}^{6}c_{ij}^2}, \tag{11}$$

where $\mathbf{ch} = [\zeta, \eta, \theta]$ is a chromosome with floating point genes representing transformation angles ζ, η and θ.

Calculated Euler angles are very low – 0.03, 0.78 and 2.32 degrees. Low values of transformation angles indicate that the considered specimen was extracted properly and main directions of orthotropy are at least roughly aligned with main anatomical axes in the human femur epiphysis. Low values of the transformation angles result in small changes in the elasticity matrix (12), but in case of bone samples extracted not properly, the procedure will noticeably improve the result.

$$\mathbf{C}_1^{\mathbf{ORT}} = \begin{bmatrix} 1894.121 & 506.982 & 567.333 & 54.833 & -25.734 & -18.961 \\ & 1682.723 & 516.523 & 39.405 & -25.161 & 2.677 \\ & & 2459.042 & 7.634 & -10.718 & -36.137 \\ & \text{sym.} & & 445.404 & -6.089 & -12.251 \\ & & & & 465.482 & 15.435 \\ & & & & & 489.611 \end{bmatrix}. \tag{12}$$

Buffer zone is used only to apply the periodic boundary conditions. To reduce the influence of the buffer zone on the calculated effective material parameters of the bone sample, the δ_{ij} elements of matrix (12) are set to zero, then matrix $\mathbf{C}$ is applied as a material parameters in buffer zone region [17] and bone structure is again homogenized. Calculations are repeated until there is no change in the resulting matrix $\mathbf{C}$.

After four iterations, the final result is obtained:

$$\mathbf{C}_4^{\mathbf{ORT}} = \begin{bmatrix} 1865.218 & 494.783 & 593.234 & 56.230 & -10.282 & -25.591 \\ & 1615.209 & 526.613 & 36.488 & -27.120 & -0.162 \\ & & 2570.908 & 22.191 & -54.685 & -41.609 \\ & & & 463.521 & -4.246 & -12.898 \\ & & & & 505.883 & 19.515 \\ & & & & & 552.863 \end{bmatrix}. \tag{13}$$

The engineering constants calculated on the basis of elasticity matrix components using Eq. (7) are as follows:

$$E_1 = 1631.245 \text{ MPa}, \qquad E_2 = 1424.951 \text{ MPa}, \qquad E_3 = 2284.254 \text{ MPa}.$$

These results can be compared with the experimental study [8]. The highest anisotropy ratio (E_3/E_2) is equal to 1.6, a relatively low value related to high BV/TV of the considered bone sample.

The compression experiment was performed for a second axis. The effective Young's modulus obtained from experiment was equal to 1148 MPa and the one obtained in numerical analysis is equal to 1424.951 MPa.

The difference between the homogenized and experimental parameters is a result of periodic boundary conditions applied in RVE model (the model is more stiff than in the experimental setup) and confirms the 20 to 40% underestimation [18] of laboratory test results. In vivo, fragment of tissue behaves in a way that is similar to the model with periodic boundary conditions (which is surrounded by tissue). This can led to an assumption that these higher values are closer to actual parameters of bone tissue as a real periodic structure.

6. Conclusions

Numerical FEM models of trabecular bone microstructure obtained on the basis of micro- tomography data segmentation along with numerical homogenization method allow to calculate effective material parameters of bone tissue. Periodic boundary conditions can be applied for RVE models with irregular boundary meshes with the use of buffer zone. The use of periodic boundary conditions resulted in higher stiffness of calculated effective parameters than the parameters obtained trough experimental compression test. Low values of calculated transformation angles indicate that anatomical axes in head of the human femur are coincident with main directions of orthotropy. The obtained orthotropic effective material parameters of bone may be used in future analyses in the areas pertaining to tissue engineering.

References

[1] M. Binkowski, G. Davis, Z. Wrobel, A. Goodship. Quantitative measurement of the bone density by X-ray micro vomputed tomography. *IFMBE Proceedings*, **31**: 856–859, 2010.

[2] T. Burczyński, W. Kuś. Microstructure optimisation and identification in multi-scale modeling. *Computational Methods in Applied Sciences*, **14**: 169–181, 2009.

[3] T. Burczyński, W. Kuś, A. Brodacka. Multiscale modeling of osseous tissues. *Journal of Theoretical and Applied Mechanics*, **48**: 855–870, 2010.

[4] S. Hollister, R. Maddox, J. Taboas. Optimal design and fabrication of scaffolds to mimic tissue properties and satisfy biological constraints. *Biomaterials*, **23**: 4095–4103, 2002.

[5] Y. Holdstein, L. Podshivalov, A. Fischer. Geometric modeling and analysis of bone micro-structures as a base for scaffold design. *Computational Methods in Applied Sciences*, **20**: 91–109, 2011.

[6] A. John, M. Duda, P. Makowski. The influence of material parameters modeling method on stress and strain state in human femur. *Proceedings of Biomechanics 2012, International conference of the Polish Society of Biomechanics*, 119–120, 2012.

[7] J. Kabel, B. Van Rietbergen, M. Dalstra, A. Odgaard, R. Huiskes. The role of an effective isotropic tissue modulus in the elastic properties of cancellous bone. *Journal of Biomechanics*, **32**: 673–680, 1999.

[8] G. Kokot. *Evaluation of bone mechanical properties using digital image correlation, nanoindentation and numerical simulations* (in Polish). Monograph 484, Silesian University of Technology, Gliwice, 2013.

[9] G. Kokot, M. Binkowski, A. John, B. Gzik-Zroska. Advanced mechanical testing methods in determining bone material properties. *Mechanika*, **18**: 139–143, 2012.

[10] S.R. Lorenzetti. New method to determine the Young's modulus of single trabeculae. *DSc Dissertation*, Zurich, 2006.

[11] Ł. Madej, A. Mrozek, W. Kuś, T. Burczyński, M. Pietrzyk. Concurrent and upscaling methods in multi-scale modelling – case studies. *Computer Methods in Material Science*, **8**: 1–15, 2008.

[12] P. Makowski. Trabecular bone homogenization with use of MSC.Marc user subroutines. *International Conference on Computer Methods in Mechanics CMM 2013 Proceedings*, Poznań, 2013.

[13] P. Makowski, A. John, W. Kuś, G. Kokot. Multiscale modeling of the simplified trabecular bone structure. *Proceedings of 18th International Conference Mechanika 2013*, 156–161, 2013.

[14] P. Makowski, W. Kuś, G. Kokot. Evolutionary identification of trabecular bone properties. *ECCOMAS International Conference IPM 2013 Proceedings*, 35–36, 2013.

[15] J. Szyndler, Ł. Madej. Effect of number of grains and boundary conditions on digital material representation deformation under plane strain. *Archives of Civil and Mechanical Engineering*, 2013.

[16] K. Terada, M. Hori, T. Kyoya, N. Kikuchi. Simulation of the multi-scale convergence in computational homogenization approaches. *International Journal of Solids and Structures*, **37**: 2285–2311, 2000.

[17] D. Trias, J. Costa, J.A. Mayugo, J.E. Hurtado. Random models versus periodic models for fibre reinforced composites. *Computational Materials Science*, **38**: 316–324, 2006.

[18] B. Van Rietbergen, R. Huiskes. Elastic constants of cancellous bone. In: Cowin, S.C. (Ed.), *Bone Mechanics Handbook, 2nd Edition*, CRC Press, Boca Raton, FL, 2001.

[19] B. Van Rietbergen, A. Odgaard, J. Kabel, R. Huiskes. Direct mechanics assessment of elastic symmetries and properties of trabecular bone architecture. *Journal of Biomechanics*, **29**: 1653–7, 1996.

[20] B. Van Rietbergen, A. Odgaard, J. Kabel, R. Huiskes. Relationships between bone morphology and bone elastic properties can be accurately quantified using high-resolution computer reconstructions. *Journal of Orthopaedic Research*, **16:** 23–28, 1998.

[21] G. Yang, J. Kabel, B. Van Rietbergen, A. Odgaard, R. Huiskes, S.C. Cowin. The anisotropic Hooke's law for cancellous bone and wood. *Journal of Elasticity*, **53**: 125–146, 1999.